

Criticality in the configuration-mixed interacting boson model: (1) $U(5)$ - $\hat{Q}(\chi) \cdot \hat{Q}(\chi)$ mixing

V. Hellemans^a, P. Van Isacker^b, S. De Baerdemacker^a and
K. Heyde^{a,c}

^a*Department of Subatomic and Radiation Physics,
Proeftuinstraat 86, B-9000 Gent, Belgium*

^b*Grand Accélérateur National d'Ions Lourds, CEA/DSM-CNRS/IN2P3,
B.P. 55027, F-14076 Caen Cedex 5, France*

^c*ISOLDE, CERN, CH-1211 Geneva 23, Switzerland*

Abstract

The case of $U(5)$ - $\hat{Q}(\chi) \cdot \hat{Q}(\chi)$ mixing in the configuration-mixed Interacting Boson Model is studied in its mean-field approximation. Phase diagrams with analytical and numerical solutions are constructed and discussed. Indications for first-order and second-order shape phase transitions can be obtained from binding energies and from critical exponents, respectively.

Key words: Interacting boson model, configuration mixing, phase transitions, critical exponents

PACS: 21.60.Fw, 21.60.Ev, 05.70.Fh, 05.70.Jh

1 Introduction

The interacting boson model (IBM) introduced by Arima and Iachello [1] is an algebraic model that has its roots in the nuclear shell model. The approximation of the IBM that only $L = 0$ and $L = 2$ nucleon pairs are considered and mapped onto s and d bosons gives rise to the group structure $U(6)$. This serves as the dynamical algebra of the model, *i.e.*, the Hamiltonian and other operators can be expressed in terms of the generators of $U(6)$. Furthermore,

Email address: veerle.hellemans@ugent.be (V. Hellemans).

the $U(6)$ group structure leads to the remarkable property that the Hamiltonian is analytically solvable for certain choices of the interaction parameters. In spite of its microscopic underpinning in terms of the shell model of the atomic nucleus, the IBM can also be linked to a macroscopic interpretation of the nucleus by means of the coherent-state formalism [2,3,4]. This formalism allows one to associate an energy surface in the collective quadrupole shape parameters β and γ with any IBM Hamiltonian. Hence, the analytically solvable limits of the Hamiltonian, the $U(5)$, $O(6)$ and $SU(3)$ limits, can be linked to a spherical vibrator, a γ -independent rotor, and a prolate or oblate deformed rotor, respectively. The evolution of the IBM Hamiltonian with varying parameters and the associated energy surface has been studied extensively [5,6,7,8,9]. It was shown that the energy surface undergoes a first-order quantum phase transition in the passage from $U(5)$ to $SU(3)$ and a second-order quantum phase transition from $U(5)$ to $O(6)$. The concept of quantum phase transitions was introduced by Gilmore *et al.* [10,11] in analogy with the well-known thermodynamic phase transitions. Quantum phase transitions are not driven by the control parameter temperature, however, but rather by the parameters of the Hamiltonian describing the quantum system. In the IBM in its simplest form the bosons are restricted to the valence space but the model can be extended to a configuration-mixed version (IBM-CM) [12,13] where particle-hole (p-h) excitations across a closed proton or neutron shell are incorporated. In certain regions of the nuclear chart these p-h excitations descend very low in energy such that they can strongly interact with the regular configuration or even become the ground state. Macroscopically this is understood as shape coexistence, the coexistence of several minima of the energy surface within a very small energy interval. This macroscopic information can be extracted from the IBM-CM by calculating the expectation value in a coherent state appropriate for configuration mixing [14]. The resulting energy surface exhibits a single minimum or several coexisting minima depending on the IBM-CM parameters. Recently, the energy surface for $U(5)$ - $O(6)$ mixing has been studied [15] and it was shown that the IBM-CM in this case gives rise to an extended phase with shape coexistence.

The aim of this paper is the study of the more general case of $U(5)$ - $\hat{Q}(\chi)\hat{Q}(\chi)$ mixing, where $\hat{Q}(\chi)$ (see sect. 2) is the quadrupole operator which drives the system to deformation and $U(5)$ is the spherical-vibrator limit of the IBM.

2 The energy surface for $U(5)$ - $\hat{Q}(\chi)\hat{Q}(\chi)$ mixing

The most compact form of the IBM Hamiltonian, which captures the essential physics of the model, is obtained within the consistent- Q formalism [16]

$$\hat{H}_{\text{cwf}} = \epsilon \hat{n}_d - |\kappa| \hat{Q}(\chi) \cdot \hat{Q}(\chi) , \quad (1)$$

where \hat{n}_d is the d -boson number operator and $\hat{Q}(\chi) = (s^\dagger \tilde{d} + d^\dagger s)^{(2)} + \chi(d^\dagger \tilde{d})^{(2)}$ the quadrupole operator. For specific choices of the parameters ϵ , κ and χ , the three symmetry limits of the IBM are obtained: the $U(5)$ limit for $\kappa=0$, the $O(6)$ limit for $\epsilon = 0$ and $\chi = 0$ and the $SU(3)$ limit for $\epsilon = 0$ and $\chi = \pm\sqrt{7}/2$. By calculating the expectation value of the Hamiltonian (1) in a normalised projective coherent state [2,3,4]

$$|N, \beta, \gamma\rangle = \frac{1}{\sqrt{N!(1+\beta^2)^{N/2}} \left(s^\dagger + \beta \left[\cos \gamma d_0^\dagger + \frac{1}{\sqrt{2}} \sin \gamma (d_2^\dagger + d_{-2}^\dagger) \right] \right)^N |0\rangle, \quad (2)$$

the associated energy surface is obtained

$$\begin{aligned} E^N(\epsilon, |\kappa|, \chi, \beta, \gamma) &\equiv \langle N, \beta, \gamma | \hat{H}_{\text{cwf}} | N, \beta, \gamma \rangle \\ &= \epsilon N \frac{\beta^2}{1+\beta^2} - |\kappa| \left[\frac{N [5 + (1 + \chi^2)\beta^2]}{1 + \beta^2} \right. \\ &\quad \left. + \frac{N(N-1)}{(1+\beta^2)^2} \left(\frac{2}{7} \chi^2 \beta^4 - 4\sqrt{\frac{2}{7}} \chi \beta^3 \cos(3\gamma) + 4\beta^2 \right) \right], \quad (3) \end{aligned}$$

where N denotes the number of valence bosons and (β, γ) are collective variables. If the values of the parameters for the three different IBM limits are inserted, it is found that the $U(5)$ limit can be associated with an energy surface with a spherical minimum, the $O(6)$ limit with one with a deformed but γ -independent minimum, and the $SU(3)$ limit with an energy surface which has either a prolate (for $\chi = -\sqrt{7}/2$) or an oblate (for $\chi = \sqrt{7}/2$) deformed minimum.

An extended version of the IBM with configuration mixing (IBM-CM) allows the simultaneous treatment and mixing of several boson configurations which correspond to different particle-hole (p-h) shell-model excitations [12,13]. In particular, configurations with N , $N+2$, $N+4$, ... bosons are associated with 0p-0h, 2p-2h, 4p-4h, ... excitations, respectively. In case of mixing between a 'regular' 0p-0h and a 'intruder' 2p-2h configuration, the Hamiltonian can be written as

$$\hat{H} = \hat{P}_N^\dagger \hat{H}_{\text{cwf}}^N \hat{P}_N + \hat{P}_{N+2}^\dagger \left(\hat{H}_{\text{cwf}}^{N+2} + \Delta \right) \hat{P}_{N+2} + \hat{V}_{\text{mix}}, \quad (4)$$

where \hat{P}_N and \hat{P}_{N+2} are operators projecting onto the N -boson and $(N+2)$ -boson spaces, respectively. Although the Hamiltonians are formally equivalent, the different superscripts in \hat{H}_{cwf}^N and $\hat{H}_{\text{cwf}}^{N+2}$ indicate that the parametrisation can be configuration dependent. The parameter Δ is the energy needed to excite two particles across a shell gap, corrected for the pairing interaction and a monopole effect [17]. Finally, $\hat{V}_{\text{mix}} \equiv w_0(s^\dagger s^\dagger + ss) + w_2(d^\dagger \cdot d^\dagger + \tilde{d} \cdot \tilde{d})$ denotes the interaction between the two configurations. This form of the Hamiltonian can be easily extended to incorporate configuration mixing with higher-order

particle-hole excitations.

The geometric interpretation of the IBM-CM is obtained by introducing a matrix coherent-state method [14]. In case of mixing between a 0p-0h and a 2p-2h configuration the energy surface is given by the lowest eigenvalue of the matrix

$$\begin{bmatrix} E^N(\epsilon_1, |\kappa_1|, \chi_1, \beta, \gamma) & \omega(\beta) \\ \omega(\beta) & E^{N+2}(\epsilon_2, |\kappa_2|, \chi_2, \beta, \gamma) + \Delta \end{bmatrix}, \quad (5)$$

with

$$\omega(\beta) \equiv \langle N, \beta, \gamma | \hat{V}_{\text{mix}} | N+2, \beta, \gamma \rangle = \sqrt{(N+2)(N+1)} \frac{w_0 + w_2 \beta^2}{1 + \beta^2}, \quad (6)$$

and $E^N(\epsilon_1, |\kappa_1|, \chi_1, \beta, \gamma)$ and $E^{N+2}(\epsilon_2, |\kappa_2|, \chi_2, \beta, \gamma)$ the expectation values of \hat{H}_{cwf}^N and $\hat{H}_{\text{cwf}}^{N+2}$ in the appropriate projective coherent state. For simplicity's sake, w_0 and w_2 are taken equal ($w_0 = w_2 \equiv w$) such that ω becomes β independent.

In the language of catastrophe theory [18], which can be used to study qualitative changes in the energy surface, $(N, \epsilon_1, |\kappa_1|, \chi_1, \epsilon_2, |\kappa_2|, \chi_2, \Delta, \omega)$ are called control parameters. Because a general study of the energy surface as a function of all nine control parameters is totally out of (current) computational reach, we focus on mixing between the dynamical symmetries of the IBM which can be considered as the benchmarks of the model. In the present paper we concentrate on the case of mixing between the vibrational $U(5)$ limit and the deformation driving quadrupole term $\hat{Q}(\chi) \cdot \hat{Q}(\chi)$ which incorporates both the $O(6)$ limit and the $SU(3)$ limit for $\chi = 0$ and $\chi = \pm\sqrt{7}/2$, respectively. In a forthcoming paper the case of mixing between deformed configurations will be treated.

The energy surface resulting from the matrix coherent-state method in the case of $U(5)$ - $\hat{Q}(\chi) \cdot \hat{Q}(\chi)$ mixing is given by

$$\begin{aligned}
E_- = & \frac{|\kappa|}{2(1+\beta^2)^2} \left(\left[\epsilon' N - (N+2)(1+\chi^2) - \frac{2}{7}(N+2)(N+1)\chi^2 + \Delta' \right] \beta^4 \right. \\
& + \left[\epsilon' N - (N+2)(6+\chi^2) - 4(N+2)(N+1) + 2\Delta' \right] \beta^2 \\
& + \frac{4}{7}(N+2)(N+1)\sqrt{14}\chi\beta^3 \cos(3\gamma) - 5(N+2) + \Delta' \\
& - \left[\left(\left[\epsilon' N + (N+2)(1+\chi^2) + \frac{2}{7}(N+2)(N+1)\chi^2 - \Delta' \right] \beta^4 \right. \right. \\
& + \left. \left. \left[\epsilon' N + (N+2)(6+\chi^2) + 4(N+2)(N+1) - 2\Delta' \right] \beta^2 \right. \right. \\
& \left. \left. - \frac{4}{7}(N+2)(N+1)\sqrt{14}\chi\beta^3 \cos(3\gamma) + 5(N+2) - \Delta' \right)^2 \right. \\
& \left. + \omega'^2(1+\beta^2)^4 \right]^{\frac{1}{2}}, \tag{7}
\end{aligned}$$

where $\Delta' = \Delta/|\kappa|$, $\epsilon' = \epsilon/|\kappa|$ and $\omega' = 2\omega/|\kappa|$. We will omit the scaling factor $|\kappa|/2$ from now on as the structural properties only depend on Δ' , ϵ' and ω' .

3 Criticality conditions and Maxwell points

3.1 Introduction

In the following we rely on the ideas of catastrophe theory as discussed extensively by Gilmore [18]. In the family of energy surfaces $E_-(\beta, \gamma; \epsilon', \chi, \Delta', \omega', N)$ under study, $(\epsilon', \chi, \Delta', \omega', N)$ are referred to as the control parameters while (β, γ) are the collective variables. In general, for an arbitrary set of control parameters $(\epsilon'_0, \chi_0, \Delta'_0, \omega'_0, N_0)$, the energy surface in (β, γ) exhibits isolated critical (or equilibrium) points. Isolated critical points are characterised by a vanishing gradient of the energy surface ($\nabla E_- = 0$) and a non-zero determinant of the stability matrix ($\det(\mathcal{S}) \neq 0$). The latter matrix is defined as

$$\mathcal{S} = \begin{bmatrix} \frac{\partial^2 E_-}{\partial \beta^2} & \frac{\partial^2 E_-}{\partial \beta \partial \gamma} \\ \frac{\partial^2 E_-}{\partial \gamma \partial \beta} & \frac{\partial^2 E_-}{\partial \gamma^2} \end{bmatrix}, \tag{8}$$

and its eigenvalues determine the stability properties of the energy surface in isolated critical points. If all the eigenvalues of \mathcal{S} are positive, the isolated critical point is a minimum; negative eigenvalues of \mathcal{S} indicate a maximum whereas positive and negative eigenvalues characterise a saddle point. Since the isolated critical points are the extrema or saddle points of the energy surface $E_-(\beta, \gamma; \epsilon'_0, \chi_0, \Delta'_0, \omega'_0, N_0)$, they determine its global behaviour. For spe-

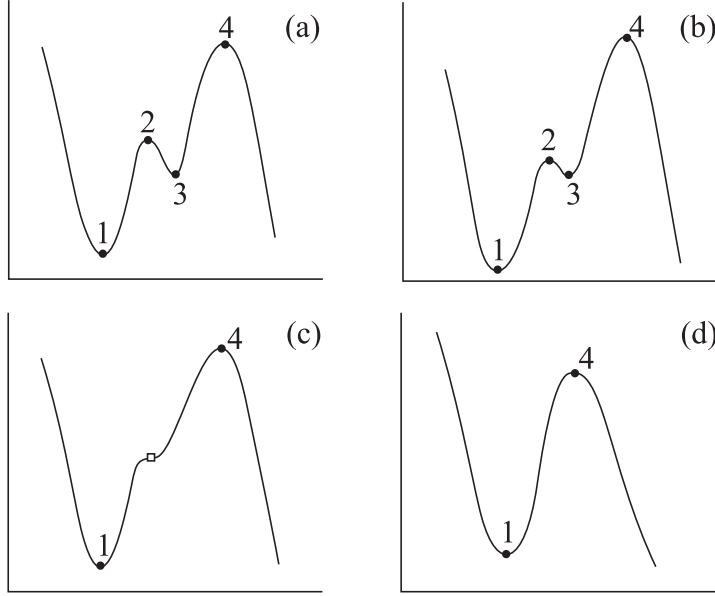


Fig. 1. Illustration of the fact that degenerate critical points organise the qualitative behaviour of a family of functions. Panels (a), (b), (c) and (d) show an arbitrary function for different sets of the control parameters. In panels (a), (b) and (d) the function exhibits only isolated critical points (indicated with a dot) while in panel (c) it has a degenerate critical point (indicated with a square). The number of isolated critical points or extrema changes when the control parameters pass through (c) corresponding to a degenerate critical point.

cific values of the control parameters the energy surface exhibits points where the determinant of the stability matrix vanishes ($\det(\mathcal{S})=0$). These are the *degenerate* critical points and they are of great importance. Whereas isolated critical points organise the qualitative behaviour of a single energy surface, degenerate critical points organise the qualitative behaviour of the entire family of energy surfaces $E_-(\beta, \gamma; \epsilon', \chi, \Delta', \omega', N)$. If the control parameters are varied and pass through values where the energy surface exhibits degenerate critical point(s), the topology of the surface changes. This can be understood intuitively by realising that the topology of an energy surface is determined by its isolated critical points. Consequently, if two or more isolated critical points merge into a single degenerate one, the topology of the energy surface changes. This is illustrated in fig. 1 where the evolution of an arbitrary function with varying control parameters is shown. In panel (a) the function exhibits 4 isolated critical points (indicated with a dot). If the control parameters are changed, two extrema (2 and 3) move towards each other (panel (b)) until they merge into a degenerate critical point (indicated with a square) in panel (c). In panel (d) the degenerate critical point has disappeared and only two extrema remain. It is clear that (c) with its degenerate critical point separates the region where the function exhibits 4 extrema from the region where it has only 2.

Summarising, the degenerate critical points mark out the different regions in

the control parameter space where the qualitative properties of the energy surface remain unchanged. Hence, they determine specific lines in the phase diagram. If two such lines in the phase diagram intersect, the degeneracy of the crossing point is higher than the degeneracy of the critical points determining the lines in the phase diagram. This crossing is called a triple point. In regions of the phase diagram where the energy surface has several minima, it is of interest to know which of these is the global minimum and where it jumps from one minimum to another (*i.e.*, where two degenerate global minima occur). The locus of points in control parameter space where this jump of the global minimum occurs is called the set of Maxwell points. In the case of $U(5)\text{-}\hat{Q}(\chi) \cdot \hat{Q}(\chi)$ mixing, the Maxwell points are the solutions of

$$\left. \frac{\partial E_-}{\partial \beta} \right|_{\beta=\beta_0} = 0, \quad E_-(\beta = \beta_0) - E_-(\beta = 0) = 0. \quad (9)$$

3.2 Analytical solution in $(\beta, \gamma) = (0, n\pi/3)$

In general, the criticality conditions

$$\frac{\partial E_-}{\partial \beta} = 0, \quad \frac{\partial E_-}{\partial \gamma} = 0, \quad \det(\mathcal{S}) = 0, \quad (10)$$

have to be solved numerically. However, an analytical solution can be found. Since mixing between spherical $U(5)$ and deformed $\hat{Q}(\chi) \cdot \hat{Q}(\chi)$ is considered, we expect important changes in the energy surface to occur at $\beta = 0$ which is a minimum in the spherical case and a maximum for the deformed case. Expanding the energy surface E_- of eq. (7) around $(\beta, \gamma) = (0, n\pi/3)$ (n integer), we find

$$E_- = t_{00} + \frac{1}{2!}t_{20}\beta^2 + \frac{1}{3!}t_{30}\beta^3 + \frac{1}{4!}t_{40}\beta^4 + \frac{1}{5!}t_{50}\beta^5 + \frac{1}{12}t_{32}\beta^3\gamma^2 + \frac{1}{6!}t_{60}\beta^6 + \dots, \quad (11)$$

with

$$\begin{aligned}
t_{00} &= -\zeta - \sqrt{\zeta^2 + \omega'^2} , \\
t_{20} &= \frac{2}{\sqrt{\zeta^2 + \omega'^2}} \left[\epsilon' N \left(\sqrt{\zeta^2 + \omega'^2} - \zeta \right) \right. \\
&\quad \left. - (N+2)(\chi^2 + 4N) \left(\sqrt{\zeta^2 + \omega'^2} + \zeta \right) \right] , \\
t_{30} &= \frac{24}{7} (N+2)(N+1) \sqrt{14} \chi \cos(n\pi) \frac{\zeta + \sqrt{\zeta^2 + \omega'^2}}{\sqrt{\zeta^2 + \omega'^2}} , \\
t_{40} &= -24 \frac{\zeta + \sqrt{\zeta^2 + \omega'^2}}{\sqrt{\zeta^2 + \omega'^2}} \left(\epsilon' N + (N+2) \left[\frac{1}{7} (2N-5)\chi^2 - 4(2N+1) \right] \right) \\
&\quad - \frac{12\omega'^2}{(\zeta^2 + \omega'^2)^{\frac{3}{2}}} \left[\epsilon' N + (N+2)(\chi^2 + 4N) \right]^2 + \frac{48\zeta\epsilon' N}{\sqrt{\zeta^2 + \omega'^2}} , \\
t_{50} &= \frac{480}{7} (N+2)(N+1) \sqrt{14} \chi \cos(n\pi) \\
&\quad \times \left[-\frac{2(\zeta + \sqrt{\zeta^2 + \omega'^2})}{\sqrt{\zeta^2 + \omega'^2}} + \omega'^2 \frac{\epsilon' N + (N+2)(\chi^2 + 4N)}{(\zeta^2 + \omega'^2)^{\frac{3}{2}}} \right] , \\
t_{32} &= -\frac{216}{7} (N+2)(N+1) \sqrt{14} \chi \cos(n\pi) \frac{\zeta + \sqrt{\zeta^2 + \omega'^2}}{\sqrt{\zeta^2 + \omega'^2}} , \tag{12}
\end{aligned}$$

where the notation $\zeta = -\Delta' + 5(N+2)$ is used.

The criticality conditions (10) are automatically fulfilled in the point $(\beta, \gamma) = (0, n\pi/3)$ as the linear terms in β and γ as well as the quadratic term γ^2 are zero. Consequently, the lines determining the phase diagram in control parameter space for $(\beta, \gamma) = (0, n\pi/3)$ are found by requiring a vanishing β^2 term in the Taylor expansion. Hence, if $t_{20} = 0$, the stability matrix \mathcal{S} vanishes identically and we obtain the locus of four-fold degenerate critical points (two-fold in β and two-fold in γ),

$$\epsilon'_c = -\frac{(N+2)(4N + \chi^2)}{N} \frac{\zeta + \sqrt{\zeta^2 + \omega_c'^2}}{\zeta - \sqrt{\zeta^2 + \omega_c'^2}} . \tag{13}$$

In case of $U(5)$ – $O(6)$ mixing one has $\chi = 0$ and the energy surface (7) will exhibit a β^4 behaviour around $(\beta, \gamma) = (0, n\pi/3)$, if the control variables are chosen according to (13). In all other cases the behaviour of the energy surface at the critical points (13) is of dominant β^3 character. Note that the global behaviour of the analytical critical line remains essentially unchanged when the intruder configuration changes from a γ -independent rotor to a prolate/oblate rotor as χ is part of a positive scaling factor. If $\zeta > 0$ or $\Delta' < 5(N+2)$, the curve converges asymptotically to the lines $\omega' = 0$ and $\epsilon' = (N+2)(4N + \chi^2)/N$. If $\Delta' = 5(N+2)$, ϵ'_c takes on the constant value $(N+2)(4N + \chi^2)/N$. If $\zeta < 0$ or $\Delta' > 5(N+2)$, only the asymptote $\epsilon' = (N+2)(4N + \chi^2)/N$ remains. As long as $\epsilon' < \epsilon'_c$, a deformed minimum is found whereas the energy surface exhibits a spherical minimum for $\epsilon' > \epsilon'_c$. If the excitation energy of the intruder state goes to infinity, $\Delta' \rightarrow \infty$, eq. (13) reduces to $\epsilon'_c = 0$.

In order to find higher-order degenerate critical points, higher-order terms are required to vanish. The coefficient t_{30} vanishes for $\chi = 0$, or for $\omega' = 0$ and $\Delta' > 5(N + 2)$, or for $\Delta' = \infty$. For $\chi = 0$ the coefficients t_{32} , t_{50} and all higher-order terms with γ dependence disappear. This can also be seen from the energy surface (7) which becomes γ independent if $\chi = 0$. If we additionally impose that $t_{40} = 0$, we find the triple point

$$(\epsilon'_t, \omega'_t) = \left(\frac{4N^2(N + 2) + \zeta(N + 1)}{N^2}, \pm \frac{4N\sqrt{(N + 2)[4N^2(N + 2) + \zeta(N + 1)]}}{N + 1} \right). \quad (14)$$

In the (ϵ', ω') plane of the control parameter space, eq. (14) gives the triple point where the analytical solution (13) for $(\beta, \gamma) = (0, n\pi/3)$ and the numerical solution of eq. (10) for $(\beta, \gamma) \neq (0, n\pi/3)$ intersect. From the Taylor expansion it is seen that the energy surface exhibits a β^6 behaviour in the vicinity of the triple point.

3.3 Numerical solutions

In the general case $(\beta, \gamma) \neq (0, n\pi/3)$, the critical points (see eq. (10)) and the Maxwell points (see eq. (9)) must be calculated numerically for the energy surface E_- in eq. (7). To simplify the numerical treatment, γ can be “frozen” to a certain $n\pi/3$. This follows from the fact that the condition $\partial E_- / \partial \gamma = 0$ implies necessarily that $\chi = 0$, $\gamma = n\pi/3$ or $\beta = 0$. The case $\beta = 0$ has already been treated in the analytical solution (sect. 3.2) and all γ dependence disappears if $\chi = 0$. If we choose $\gamma = n\pi/3$, $\partial^2 E_- / \partial \gamma^2$ is positive definite as long as γ and the sign of χ and β are chosen consistently.¹ Hence, γ can be fixed to $n\pi/3$ without loss of generality and the criticality conditions reduce to

$$\frac{\partial E_-}{\partial \beta} = \frac{\partial^2 E_-}{\partial \beta^2} = 0. \quad (15)$$

In the following sections, we choose $\gamma = 0$.

4 Phase diagrams for $U(5)$ - $Q(\chi) \cdot Q(\chi)$ mixing

In sect. 3.2 we have shown that χ is part of a positive scaling factor in the analytical solution of the criticality conditions. The criticality conditions cannot

¹ If $\gamma=0$, χ must be negative and $\beta \geq 0$. If $\gamma = \pi/3$, a positive sign for χ and β must be chosen.

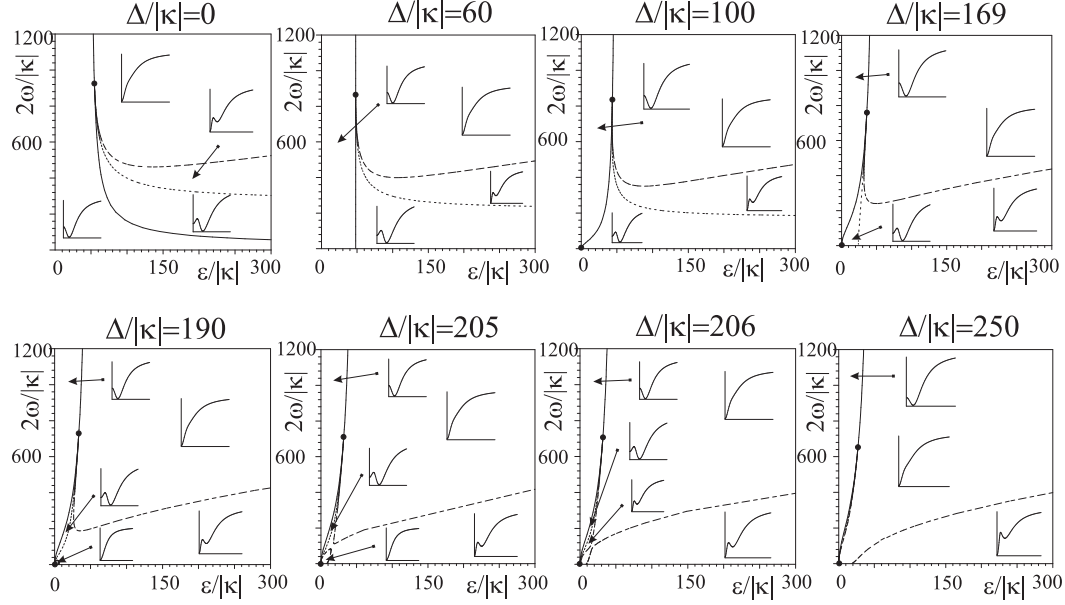


Fig. 2. Phase diagrams in the case of $U(5)$ – $O(6)$ mixing for several values of Δ' and for $N = 10$. The locus of analytical critical points is shown as a full line, that of numerical critical points as a dashed line and that of Maxwell critical points as a dotted line. The dots represent triple points. The inset figures illustrate the generic shape of the potential as a function of β in each of the zones of the parameter space.

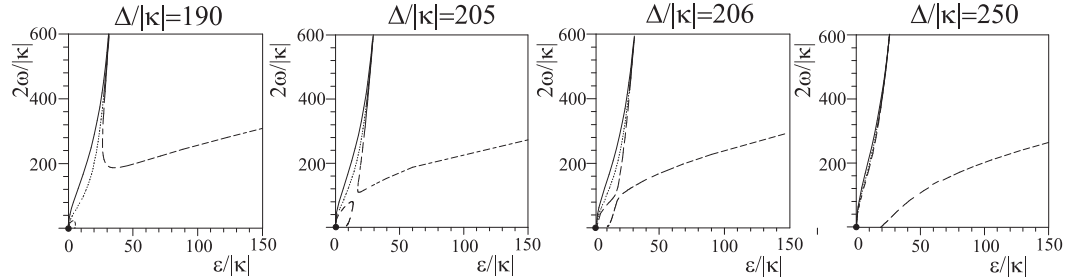


Fig. 3. Zoom on the part near the origin of the phase diagrams shown in fig. 2. The locus of analytical critical points is shown as a full line, that of numerical critical points as a dashed line and that of Maxwell critical points as a dotted line.

be solved in general if χ is considered as a symbolic parameter but they can if a specific value of χ is taken. In this section we discuss the two benchmark cases, namely $U(5)$ – $O(6)$ and $U(5)$ – $SU(3)$ mixing.

4.1 $U(5)$ – $O(6)$ mixing

The case of $U(5)$ – $O(6)$ mixing is obtained by choosing $\chi = 0$ in eq. (7). In figs. 2 and 3 different phase diagrams are shown for several values of Δ' . The number of bosons is $N = 10$. For $\Delta' = 0$ we note a deformed region to the left of the analytical solution (full line), a spherical region to the right and

above the numerical solution (dashed line) and a region of shape coexistence in between the two lines. These three regions meet in the triple point, indicated by a dot. As Δ' increases, the slope of the analytical solution switches sign and a second triple point in the origin is created. The first triple point moves down the analytical curve until it merges with the triple point in the origin $(\epsilon'_t, \omega'_t) = (0, 0)$ for $\Delta' = [4N^2(N + 2)/(N + 1)] + 5(N + 2)$ (see eq. (14)) and eventually disappears. When the slope of the Maxwell curve (dotted line) switches sign, a small spherical region for low ϵ' values starts growing around the origin. As Δ' increases further, the two spherical regions approach each other. When these two regions coalesce, the region of shape coexistence is split in two. The small coexistence region disappears when the two triple points merge, while the large coexistence region with a spherical global minimum shifts towards higher ϵ' for increasing Δ' . The evolution of the phase diagrams is similar for all N , although the value of Δ' where changes occur varies slightly with N .

4.2 $U(5)$ - $SU(3)$ mixing

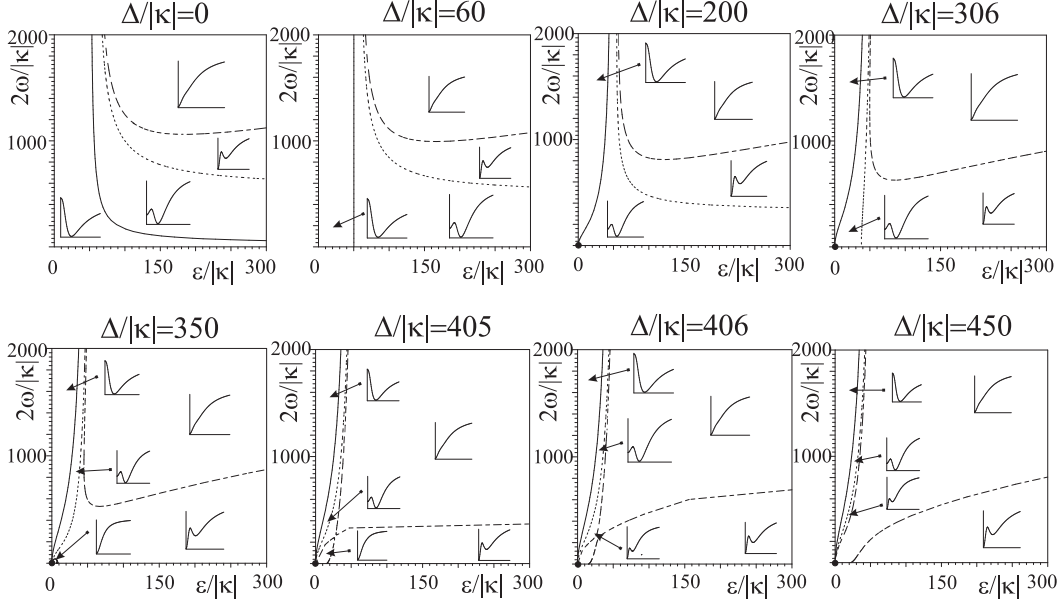


Fig. 4. Phase diagrams in the case of $U(5)$ - $SU(3)$ mixing for several values of Δ' and for $N = 10$. The locus of analytical critical points is shown as a full line, that of numerical critical points as a dashed line and that of Maxwell critical points as a dotted line. The inset figures illustrate the generic shape of the potential as a function of β in each of the zones of the parameter space.

The phase diagrams obtained in the case of $U(5)$ - $SU(3)$ mixing ($\chi = -\sqrt{7}/2$), shown in fig. 4, are very similar to those obtained for $U(5)$ - $O(6)$ mixing. It is important to note the following major differences, however. As the non-trivial triple point ($\omega'_t \neq 0$) has been proven to occur only for $\chi = 0$, the

critical (dashed and full) lines separating the different regions never meet in a triple point. This has consequences for the occurrence of shape coexistence at realistic values of the parameters when the intruder states lie very high in excitation energy. In principle, the small region of shape coexistence for low ϵ' values will only disappear if Δ' goes to infinity. Hence, even for very high excitation energies of the intruder states, there will always be a region of shape coexistence, however small, for realistic values of ϵ' and ω' . This is an essential difference with the case of $U(5)$ – $O(6)$ mixing.

5 Phase transitions

Similar to the Ehrenfest classification for thermodynamic phase transitions, a classification for shape or quantum phase transitions has been proposed [19]. The criterion involves the energy of the global minimum E_{\min} as a function of a control parameter. A shape phase transition is called of zeroth order if E_{\min} changes discontinuously at the critical point. If the first derivative of E_{\min} with respect to the order parameter or its second derivative is discontinuous at the critical point, the shape phase transition is of first or second order, respectively. The first-order phase transitions are characterised by mixed phase regimes, *i.e.* regimes where different phases coexist during the transition. Typical for second-order phase transitions is the transition from an ordered to a disordered phase or *vice versa*.

5.1 First-order phase transitions

It has been shown that the energy surface associated with the IBM (without configuration mixing) undergoes a first-order shape phase transition in the passage from $U(5)$ to $SU(3)$ [3,20]. This first-order shape phase transition occurs when passing through the small region of shape coexistence along the transition path. However, this type of shape coexistence is different from the one occurring in the phase diagrams shown here, as the latter is the result of mixing between regular and intruder configurations. Nevertheless, although the underlying physics differs, the similarities in the associated topology suggest that first-order phase transitions should also occur here when passing through the zone of shape coexistence.

In the left panel of fig. 5 is shown the energy of the extrema of the energy surface (7) and of the exact ground state of the IBM-CM Hamiltonian (also called the local term of the binding energy [21]) as a function of ω' for $N = 10$ bosons, $\Delta' = 0$, $\epsilon' = 150$, $\kappa = -0.01$ MeV and $\chi = 0$, which corresponds to the case of $U(5)$ – $O(6)$ mixing. The middle panel displays the first derivative with respect to ω' of these quantities for the same values of the other control pa-

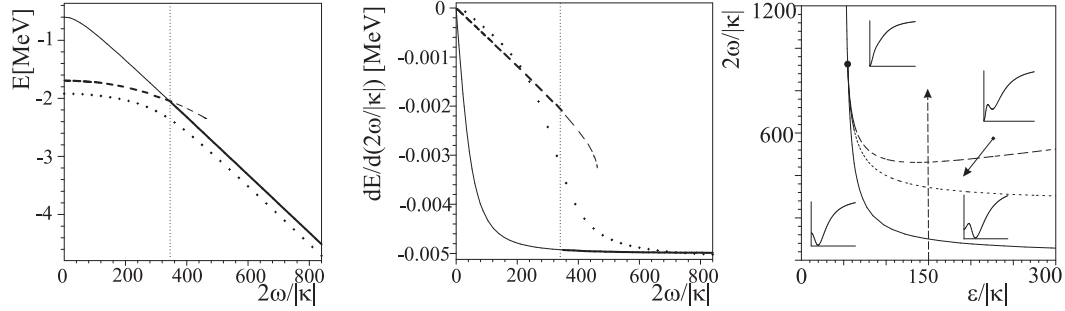


Fig. 5. Left panel: Energy of the extrema of the potential (7) and of the exact ground state of the IBM-CM Hamiltonian (1) as a function of ω' for $N = 10$ bosons, $\Delta' = 0$, $\epsilon' = 150$, $\kappa = -0.01$ MeV and $\chi = 0$. The full line corresponds to the energy of the spherical extremum (minimum or maximum at $\beta_0 = 0$) and the dashed line to the energy of the deformed minimum ($\beta_0 \neq 0$). The global minimum is indicated by a thick line. The dots show the evolution of the exact ground-state energy and the thin vertical dotted line indicates where the Maxwell line is crossed. Middle panel: The first derivative with respect to ω' of the energies shown on the left. The same conventions apply. Right panel: The (ϵ', ω') phase diagram with the transition path followed in left and middle panels.

rameters. The right panel shows the path followed in the transition. The local term of the binding energy gives the absolute energy of the 0^+ ground state. To obtain the total binding energy in the IBM, one must also include terms in the Hamiltonian which depend only on the number of bosons N [1,21]. As these terms are constant for a given N , they do not influence the phase diagram and a study of the local term of the binding energy is sufficient. In the left and middle panels the full (dashed) lines correspond to the spherical (deformed) extrema. From the crossing of the full and the dashed line in the left panel of fig. 5, it is clear that the global minimum is deformed until the transition path crosses the Maxwell line where the spherical extremum becomes lowest. Although the coherent-state formalism can be regarded as a variational mean-field method, the exact binding energies cannot be compared directly with the energy of the global minimum of the energy surface. This is due to the choice of the coherent state which does not carry exact angular momentum $L = 0$. Therefore, the coherent state breaks the $O(3)$ symmetry of the Hamiltonian which is respected in its exact diagonalisation [2]. Hence, rather than an exact, quantitative comparison of the energies, the purpose of fig. 5 is to reveal qualitative similarities along the transition path. For a quantitative comparison with the exact ground-state energies, the energy surface (7) must be projected onto $L = 0$. From fig. 5 it is clear that the exact ground-state energy and the energy of the global minimum evolve similarly with changing control parameter ω' . The middle panel of fig. 5 illustrates that the derivative of energy of the global minimum (thick line) exhibits a discontinuity at the Maxwell line where the energy surface thus undergoes a first-order shape phase transition. Since the derivative of the exact ground-state energy is reasonably close to the derivative of the global minimum and changes rapidly in the neighbourhood of

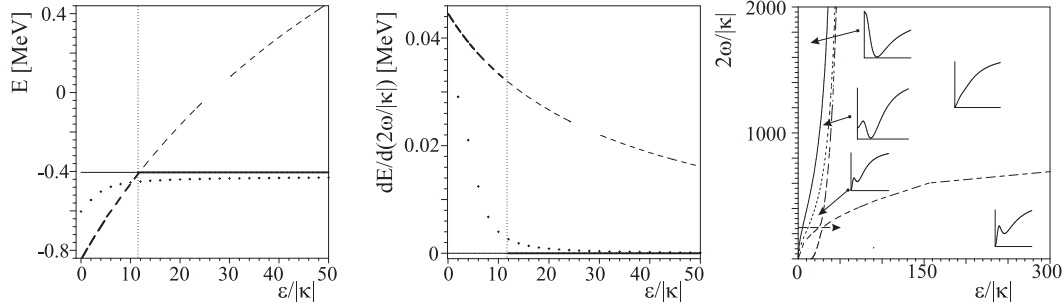


Fig. 6. Left panel: Energy of the extrema of the potential (7) and of the exact ground state of the IBM-CM Hamiltonian (1) as a function of ϵ' for $N = 10$ bosons, $\Delta' = 406$, $\omega' = 250$, $\kappa = -0.01$ MeV and $\chi = -\sqrt{7}/2$. The full line corresponds to the energy of the spherical extremum (minimum or maximum at $\beta_0 = 0$) and the dashed line to the energy of the deformed minimum ($\beta_0 \neq 0$). The global minimum is indicated by a thick line. The dots show the evolution of the exact ground-state energy and the thin vertical dotted line indicates where the Maxwell line is crossed. Middle panel: The first derivative with respect to ϵ' of the energies shown on the left. The same conventions apply. Right panel: The (ϵ', ω') phase diagram with the transition path followed in left and middle panels.

the Maxwell point, we may associate this jump in the derivative of the binding energy with a first-order shape phase transition. Summarising, in the case of $U(5)$ – $O(6)$ mixing, the nuclear system undergoes a first-order quantum phase transition when passing through the line of Maxwell points.

The same conclusion is reached for $U(5)$ – $SU(3)$ mixing. In the left panel of fig. 6 is shown the energy of the extrema of the potential surface (7) and of the exact ground state of the IBM-CM Hamiltonian as a function of ϵ' for $N = 10$ bosons, $\Delta' = 406$, $\omega' = 250$, $\kappa = -0.01$ MeV and $\chi = -\sqrt{7}/2$, which corresponds to the case of $U(5)$ – $SU(3)$ mixing. The middle panel displays the first derivative with respect to ϵ' of these quantities for the same values of the other control parameters. The right panel shows the path followed in the transition. In fig. 6 the same conventions are followed as in fig. 5; in particular, in the left and middle panels the full (dashed) lines correspond to the spherical (deformed) extrema. Note that the energies and their derivatives are studied as a function of ϵ' whereas the varying control parameter in the case of $U(5)$ – $O(6)$ mixing was ω' . The fact that the energy surface needs to be projected on $L = 0$ for a quantitative comparison with the exact energies to be valid, is immediately clear from the left panel of fig. 6. In the deformed region for small ϵ' , the exact energy is higher than the energy of the deformed minimum. This can be understood by realising that the deformation-driving part of the coherent state is also the $O(3)$ -symmetry breaking part. Hence, the need for restoring the $O(3)$ symmetry by means of angular momentum projection is largest in the deformed region. Nevertheless, the global behaviour of the exact energy and the energy of the global minimum is similar. The discontinuity in the derivative of the energy of the latter (see middle panel of fig. 6) again leads to the conclusion that the energy surface undergoes a first-order phase

transition when passing through the Maxwell point. Similarly, the slope of the derivative of the exact energy changes strongly in the neighbourhood of the Maxwell point and can be associated with a first-order shape phase transition of the energy surface. Note that the curve for the deformed minimum exhibits a gap corresponding to the passage through the narrow region with a single spherical minimum in the phase diagram for $\Delta' = 406$.

The cases discussed above are specific examples and can be repeated for any set of control parameters passing through a region with shape coexistence.

5.2 Second-order phase transitions

In the case of only one configuration, it is known that the transition from $U(5)$ to $SU(3)$ is characterised by a first-order shape phase transition. The transition from $U(5)$ to $O(6)$ on the other hand is of second order [3,20] As the energy surface associated with the IBM-CM exhibits a similar transition in the case of $U(5)$ – $O(6)$ mixing, one expects this transition to be of second order. Second-order shape phase transition are recognised from the discontinuity in the second derivative of the energy of the global minimum with respect to a control parameter. Unfortunately, an analysis similar to the one for first-order shape phase transitions experiences numerical difficulties in the neighbourhood of a critical point. Therefore, we use a different method to identify this transition. It is possible to recognise second-order phase transitions by the observation of a power law behaviour of physical quantities when passing through a critical point. In general, a power law describes the power behaviour of a physical quantity in the neighbourhood of the critical point,

$$F \sim |a_c - a|^\delta \quad (16)$$

where F is an order parameter (observable) of the system, a is a control parameter, a_c the value of the control parameter at the critical point and δ a critical exponent. This behaviour is a fingerprint of second-order phase transitions and it is a remarkable fact that phase transitions arising in different physical systems often possess the same set of critical exponents. This phenomenon is known as universality.

For the specific case of phase diagrams in configuration-mixed systems, we study the evolution of the deformation β_0 at the global minimum of the energy surface as a function of the control parameters [8]. We do this for $U(5)$ – $O(6)$ mixing and calculate the relevant critical exponents. The main reason for the choice of this order parameter is that the evolution of β_0 can be treated analytically.

The value of β_0 at the global minimum results from solving $\partial E_- / \partial \beta = 0$ in the unknowns $(\beta, \Delta', \epsilon', \omega', N)$. This equation gives rise to the following relation between the control and order parameters:

$$\omega'_{\pm} = \pm \frac{4\sqrt{-(1+\beta^2)\epsilon'N(N+2)[(N+2)\beta^2 - N]}}{(1+\beta^2)^2([\epsilon'N + 4(N+2)^2]\beta^2 + N[\epsilon' - 4(N+2)])} \\ \times \left([\epsilon'N - 4(N+2) + \zeta]\beta^4 + [\epsilon'N + 4N(N+2) + 2\zeta]\beta^2 + \zeta \right). \quad (17)$$

This relation is derived in Appendix A. Since the critical points separating the spherical and deformed phases are situated on the locus of analytically obtained critical points (13), we focus our attention on the point $\beta = 0$ and $\epsilon' = \epsilon'_c$ (see eq. (13)). For $\zeta \neq 0$ (and thus $\epsilon'_c \neq 4(N+2)$) ω'_{\pm} is continuous in the point $\beta = 0$ and $\epsilon' = \epsilon'_c$. Hence, the sign of ω'_{\pm} in $(\beta = 0, \epsilon' = \epsilon'_c)$ remains unchanged in a sufficiently small region around $(\beta = 0, \epsilon' = \epsilon'_c)$. In this point ω'_{\pm} reduces to

$$\omega'_{\pm}(\beta = 0, \epsilon' = \epsilon'_c) = \pm \frac{4\zeta\sqrt{\epsilon'_c(N+2)}}{\epsilon'_c - 4(N+2)}, \quad (18)$$

Because $\epsilon' = 4(N+2)$ is the vertical asymptote in the case of $U(5)-O(6)$ mixing, $\epsilon'_c < 4(N+2)$ if $\zeta < 0$ and $\epsilon'_c > 4(N+2)$ if $\zeta > 0$ (See sect. 3.2). Hence, in the neighbourhood of $(\beta = 0, \epsilon' = \epsilon'_c)$ ω'_+ is positive. Expanding ω'_+ around $(\beta = 0, \epsilon' = \epsilon'_c)$, we find to lowest order

$$\omega'_+ = \omega'_+(\beta = 0, \epsilon' = \epsilon'_c) + \left. \frac{\partial \omega'_+}{\partial \beta} \right|_{\beta=0, \epsilon'=\epsilon'_c} \beta + \left. \frac{\partial \omega'_+}{\partial \epsilon'} \right|_{\beta=0, \epsilon'=\epsilon'_c} (\epsilon' - \epsilon'_c) \\ + \frac{1}{2} \left. \frac{\partial^2 \omega'_+}{\partial \beta^2} \right|_{\beta=0, \epsilon'=\epsilon'_c} \beta^2 + \frac{1}{2} \left. \frac{\partial^2 \omega'_+}{\partial \epsilon'^2} \right|_{\beta=0, \epsilon'=\epsilon'_c} (\epsilon' - \epsilon'_c)^2 + \left. \frac{\partial^2 \omega'_+}{\partial \beta \partial \epsilon'} \right|_{\beta=0, \epsilon'=\epsilon'_c} (\epsilon' - \epsilon'_c) \beta \\ = \frac{4\zeta\sqrt{\epsilon'_c(N+2)}}{\epsilon'_c - 4(N+2)} - \frac{2\zeta(N+2)[4(N+2) + \epsilon'_c]}{\sqrt{\epsilon'_c(N+2)}[4(N+2) - \epsilon'_c]^2} (\epsilon' - \epsilon'_c) \\ - \frac{4\epsilon'_c(N+2)[4(N+2) + \epsilon'_c][4N^2(N+2) + \zeta(N+1) - \epsilon'_c N^2]}{N\sqrt{\epsilon'_c(N+2)}[4(N+2) - \epsilon'_c]^2} \beta^2. \quad (19)$$

If we invert relation (13) such that ω'_c becomes a function of ϵ'_c , we obtain

$$\omega'_c = \pm \frac{4\zeta\sqrt{\epsilon'_c(N+2)}}{\epsilon'_c - 4(N+2)}. \quad (20)$$

Again, ω'_c with the overall plus-sign is positive. If we substitute the positive ω'_c in expression (19), it is clear that ω'_c and the term $\omega'_+(\beta = 0, \epsilon' = \epsilon'_c)$ cancel and expression (19) reduces to

$$\frac{4\epsilon'_c(N+2)[4(N+2) + \epsilon'_c][4N^2(N+2) + \zeta(N+1) - \epsilon'_c N^2]}{N\sqrt{\epsilon'_c(N+2)}[4(N+2) - \epsilon'_c]^2} \beta^2 = \\ \frac{2\zeta(N+2)[4(N+2) + \epsilon'_c]}{\sqrt{\epsilon'_c(N+2)}[4(N+2) - \epsilon'_c]^2} (\epsilon'_c - \epsilon'). \quad (21)$$

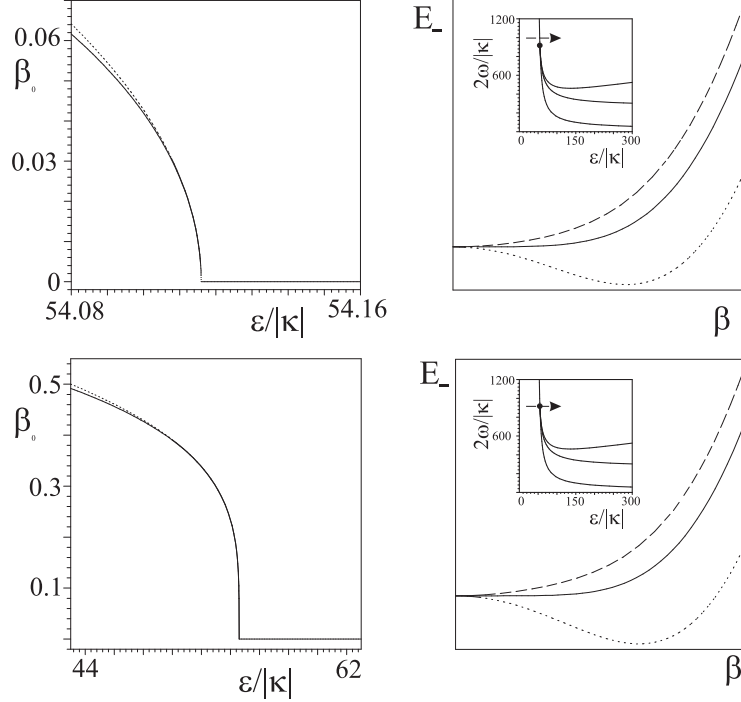


Fig. 7. Power law behaviour at the critical point (upper panels) and at the triple point (lower panels). The left panels shows the deformation at minimum, β_0 , as a function of ϵ' as predicted by the power law (dotted line) and as compared with a numerical calculation (full line). The right panels show the energy surface as a function of β , where the dotted line corresponds to $\epsilon' < \epsilon'_c$ or ϵ'_t , the full line to ϵ' at the critical or triple point, and the dashed line to $\epsilon' > \epsilon'_c$ or ϵ'_t . The inset plots indicate the transition path in the phase diagram. Other control parameters are $N = 10$, $\Delta' = 0$, and $\omega' = 1000$ (upper panels) or $\omega' = \omega'_t \approx 930.7954$ (lower panels).

We conclude that the deformed minimum occurs with deformation

$$\beta_0 = \sqrt{\frac{\zeta N}{2\epsilon'_c [4N^2(N+2) + \zeta(N+1) - \epsilon'_c N^2]}} (\epsilon'_c - \epsilon')^{1/2} \quad \text{for } \omega'_c > \omega'_t \text{ and } \epsilon' < \epsilon'_c, \quad (22)$$

in the neighbourhood of the critical point $(\epsilon'_c, \omega'_c, \Delta', N)$. The conditions $\omega'_c > \omega'_t$ and $\epsilon' < \epsilon'_c$ ensure that the deformation β_0 is real. It is clear that in the neighbourhood of the critical point $(\epsilon'_c, \omega'_c, \Delta', N)$, the deformation β_0 at the deformed minimum exhibits a power law behaviour with a critical exponent $1/2$.

If $\zeta = 0$ then ϵ'_c takes the constant value $4(N+2)$, such that ω'_\pm in (17) is discontinuous in $(\beta = 0, \epsilon' = \epsilon'_c)$. From appendix A, it follows that ω' is undefined in $(\beta = 0, \epsilon' = \epsilon'_c)$, hence, it is not possible to derive an analytical expression for the powerlaw.

In the upper panels of fig. 7 the deformation at minimum, β_0 , is shown for $N = 10$ bosons, $\omega' = 1000$ and $\Delta' = 0$ as ϵ' crosses the critical line of second

order. The evolution of β_0 in the neighbourhood of the critical point is compared with a power law with critical exponent 1/2 as obtained in (22) in the left panel. The energy surfaces just before and just after crossing the critical point as well as at the critical point are shown in the right upper panel. The inset figure shows the path followed in the phase diagram. The comparison of the power law (22) and the exact β_0 demonstrates the validity of the former in the neighbourhood of the critical point.

In the triple point itself (see eq. (14)) the coefficient of β^2 in the Taylor expansion of ω'_+ in (17) vanishes and higher-order terms have to be considered. If $\zeta \neq 0$, the Taylor expansion around $\beta = 0, \epsilon' = \epsilon'_t$ becomes to lowest order in β and $\epsilon' - \epsilon'_t$

$$\omega'_+ = a_{00} + a_{01}(\epsilon' - \epsilon'_t) + a_{02}(\epsilon' - \epsilon'_t)^2 + a_{21}(\epsilon' - \epsilon'_t)\beta^2 + a_{03}(\epsilon' - \epsilon'_t)^3 + a_{40}\beta^4, \quad (23)$$

where

$$\begin{aligned} a_{00} &= \frac{4N}{N+1} \sqrt{(N+2)[4N^2(N+2) + \zeta(N+1)]}, \\ a_{01} &= -\frac{2N^3(N+2)[8N^2(N+2) + \zeta(N+1)]}{\zeta(N+1)^2 \sqrt{(N+2)[4N^2(N+2) + \zeta(N+1)]}}, \\ a_{02} &= \frac{N^5(N+2)^2 \left(3[8N^2(N+2) + \zeta(N+1)]^2 - 64N^4(N+2)^2 \right)}{2\zeta^2(N+1)^3 \left((N+2)[4N^2(N+2) + \zeta(N+1)] \right)^{3/2}}, \\ a_{21} &= \frac{4(N+2)^2 N^2 [8N^2(N+2) + \zeta(N+1)][4N^2(N+2) + \zeta(N+1)]^2}{\zeta^2(N+1)^2 \left((N+2)[4N^2(N+2) + \zeta(N+1)] \right)^{3/2}}, \\ a_{03} &= -\frac{N^7(N+2)^3}{4\zeta^3(N+1)^4 \left((N+2)[4N^2(N+2) + \zeta(N+1)] \right)^{5/2}} \\ &\quad \times \left(5[8N^2(N+2) + \zeta(N+1)]^3 - 64N^4(N+2)^2 [5\zeta(N+1) + 24N^2(N+2)] \right), \\ a_{40} &= -\frac{6(N+2)^2 [8N^2(N+2) + \zeta(N+1)][4N^2(N+2) + \zeta(N+1)]^2}{N\zeta \left((N+2)[4N^2(N+2) + \zeta(N+1)] \right)^{3/2}}. \quad (24) \end{aligned}$$

For $\omega' = \omega'_t$ the left-hand side of eq. (23) cancels with a_{00} and the resulting equation can be solved as a quadratic equation in β^2 . Keeping only the leading term in $(\epsilon' - \epsilon'_t)$, we derive the following expression for the deformation β_0 at the minimum in the neighbourhood of the triple point:

$$\beta_0 = \left(\frac{a_{01}}{a_{40}} \right)^{1/4} (\epsilon'_t - \epsilon')^{1/4}, \quad (25)$$

$$= \left(\frac{N^4}{3(N+1)^2 [4N^2(N+2) + \zeta(N+1)]} \right)^{1/4} (\epsilon'_t - \epsilon')^{1/4}. \quad (26)$$

Thus, at the triple point the critical exponent changes from $1/2$ to $1/4$. The behaviour of β_0 at the triple point and its comparison with the power law of eq. (26) is shown in the lower panels of fig. 7. Again, the comparison is very good. Note that the critical exponents for the order parameter β_0 are the same as those in Landau theory of tricritical points [22].

6 Conclusion

In the past years, many theoretical and experimental studies have focused on the subject of quantum phase transitions in atomic nuclei. The interacting boson model provides a tractable framework to study quantum phase transitions from a theoretical point of view. Because of the algebraic foundations of the model, an energy surface is easily constructed and can be studied within the framework of catastrophe theory allowing its qualitative study as a function of the control parameters.

In the present work a detailed study of the energy surface associated with configuration mixing between a spherical $U(5)$ and a deformed $\hat{Q}(\chi) \cdot \hat{Q}(\chi)$ configuration was performed. By expanding the energy surface around $(\beta, \gamma) = (0, n\pi/3)$ we have derived an analytical solution of the criticality conditions. An analytical expression for the triple point was obtained and it was shown that it only occurs in the case of $U(5)$ – $O(6)$ mixing. For general $\beta \neq 0$ the criticality conditions must be solved for numerically. The same holds for the Maxwell points which indicate where the global minimum jumps from one deformation to another. Phase diagrams for the two most symmetrical cases of $U(5)$ – $O(6)$ and $U(5)$ – $SU(3)$ mixing have been constructed and discussed. Both cases display a large region of shape coexistence for a broad range of excitation energies of the intruder configuration. For very high excitation energies the presence of the triple point in the case of $U(5)$ – $O(6)$ implies the disappearance of the region of shape coexistence for low $\epsilon/|\kappa|$ whereas this region is always present for other deformed intruder configurations (*i.e.*, for $\chi \neq 0$). Finally, we have discussed the order of the shape phase transitions. It turns out that, generally, the derivative of the energy of the global minimum of the energy surface changes discontinuously at the Maxwell line and undergoes a first-order shape phase transition. In a numerical calculation the derivative of the binding energy follows this behaviour although the discontinuity is smoothed out because of finite-size effects. For the transition from a spherical to a deformed minimum in the case of $U(5)$ – $O(6)$ mixing, we have shown that the deformation β_0 of the global minimum exhibits a power-law behaviour in the neighbourhood of the critical point and we have given analytical expressions for the critical exponents. Hence this transition is of second order.

Acknowledgements

The authors are grateful to A. Frank, P. Cejnar and J. Ryckebusch for interesting discussions. Financial support from the “FWO-Vlaanderen” (V.H and K.H.) and the University of Ghent (S.D.B. and K.H.) which made this research possible, is acknowledged. V.H. and S.D.B. also received financial support from the European Union under contract No 2000-00084. K.H. likes to thank the ISOLDE group for their hospitality during the final stage of this work.

A Analytical solution of $\partial E_-/\partial\beta = 0$ in the case of $U(5)$ – $O(6)$ mixing

In this appendix we derive the expression (17) which results from solving the condition $\partial E_-/\partial\beta = 0$. Substituting $\chi = 0$, $\Delta' = -\zeta + 5(N + 2)$, $\omega' = 2\omega/|\kappa|$ and

$$\begin{aligned} a_1 &= \epsilon' N + 4(N + 2) - \zeta , \\ a_2 &= \epsilon' N - 4N(N + 2) - 2\zeta , \\ b_1 &= \epsilon' N - 4(N + 2) + \zeta , \\ b_2 &= \epsilon' N + 4N(N + 2) + 2\zeta , \end{aligned} \tag{A.1}$$

in the expression for the energy surface (7), we find

$$E_- = \frac{|\kappa|}{2(1 + \beta^2)^2} \left(a_1\beta^4 + a_2\beta^2 - \zeta - \left[(b_1\beta^4 + b_2\beta^2 + \zeta)^2 + \omega'^2(1 + \beta^2)^4 \right]^{\frac{1}{2}} \right). \tag{A.2}$$

Upon a scaling factor $|\kappa|/2$ the first derivative $\partial E_-/\partial\beta$ can be written as

$$\begin{aligned} \frac{\partial E_-}{\partial\beta} &= -\frac{4\beta}{(1 + \beta^2)^3} \left(a_1\beta^4 + a_2\beta^2 - \zeta - \left[(b_1\beta^4 + b_2\beta^2 \right. \right. \\ &\quad \left. \left. + \zeta)^2 + \omega'^2(1 + \beta^2)^4 \right]^{\frac{1}{2}} \right) + \frac{4a_1\beta^3 + 2a_2\beta}{(1 + \beta^2)^2} \\ &\quad - \frac{(b_1\beta^4 + b_2\beta^2 + \zeta)(4b_1\beta^3 + 2b_2\beta) + 4\omega'^2(1 + \beta^2)^3\beta}{(1 + \beta^2)^2 \left[(b_1\beta^4 + b_2\beta^2 + \zeta)^2 + \omega'^2(1 + \beta^2)^4 \right]^{\frac{1}{2}}}. \end{aligned} \tag{A.3}$$

This expression can be rewritten to

$$\begin{aligned} \frac{\partial E_-}{\partial \beta} &= \frac{2\beta}{(1 + \beta^2)^3 [(b_1\beta^4 + b_2\beta^2 + \zeta)^2 + \omega'^2(1 + \beta^2)^4]^{\frac{1}{2}}} \\ &\times \left(\left[(2a_1 - a_2)\beta^2 + (a_2 + 2\zeta) \right] [(b_1\beta^4 + b_2\beta^2 + \zeta)^2 + \omega'^2(1 + \beta^2)^4]^{\frac{1}{2}} \right. \\ &\quad \left. + (b_1\beta^4 + b_2\beta^2 + \zeta) [(b_2 - 2b_1)\beta^2 + (-b_2 + 2\zeta)] \right). \end{aligned} \quad (\text{A.4})$$

Assuming that $(2a_1 - a_2)\beta^2 + (a_2 + 2\zeta) \neq 0$ and $\beta \neq 0$, the condition $\partial E_- / \partial \beta = 0$ leads to

$$\begin{aligned} \omega'^2(1 + \beta^2)^4 &= \frac{(b_1\beta^4 + b_2\beta^2 + \zeta)^2 [(2b_1 - b_2)\beta^2 + (b_2 - 2\zeta)]^2}{[(2a_1 - a_2)\beta^2 + (a_2 + 2\zeta)]^2} \\ &\quad - (b_1\beta^4 + b_2\beta^2 + \zeta)^2, \end{aligned} \quad (\text{A.5})$$

This can be rewritten as

$$\begin{aligned} \omega'^2 &= \frac{(b_1\beta^4 + b_2\beta^2 + \zeta)^2}{(1 + \beta^2)^4 [(2a_1 - a_2)\beta^2 + (a_2 + 2\zeta)]^2} \left([2(b_1 - a_1) - (b_2 - a_2)]\beta^2 \right. \\ &\quad \left. + (b_2 - a_2 - 4\zeta) \right) \left([2(b_1 + a_1) - (b_2 + a_2)]\beta^2 + (b_2 + a_2) \right). \end{aligned} \quad (\text{A.6})$$

Inserting the expressions for a_1, a_2, b_1 and b_2 , we find eq. (17):

$$\begin{aligned} \omega'_{\pm} &= \pm \frac{4\sqrt{-(1 + \beta^2)\epsilon'N(N + 2)[(N + 2)\beta^2 - N]}}{(1 + \beta^2)^2 \left([\epsilon'N + 4(N + 2)^2]\beta^2 + N[\epsilon' - 4(N + 2)] \right)} \\ &\quad \times \left([\epsilon'N - 4(N + 2) + \zeta]\beta^4 + [\epsilon'N + 4N(N + 2) + 2\zeta]\beta^2 + \zeta \right). \end{aligned} \quad (\text{A.7})$$

If $\beta = 0$, the condition $\partial E_- / \partial \beta = 0$ is automatically fulfilled. Hence, there is always an extremum, either a minimum or a maximum, at $\beta_0 = 0$. Finally, if $(2a_1 - a_2)\beta^2 + (a_2 + 2\zeta) = 0$, it follows that

$$\epsilon'_i = -\frac{4(N + 2)[(N + 2)\beta_i^2 - N]}{N(1 + \beta_i^2)}. \quad (\text{A.8})$$

Inserting this relation in $\partial E_- / \partial \beta = 0$, we derive the following expression for ζ from the condition $(b_1\beta^4 + b_2\beta^2 + \zeta) = 0$ (see eq. A.4)

$$\zeta_i = \frac{4(N + 2)\beta_i^2[(N + 3)\beta_i^2 - 2N]}{(1 + \beta_i^2)^2}. \quad (\text{A.9})$$

The index i has been added to demonstrate that ϵ_i, β_i and ζ_i cannot be varied independently. The parameter ω' however can take on any value. Hence, for a given ζ_i , there is a corresponding ϵ_i for which the deformation β_i of the

extremum of the energy surface remains unchanged when ω' is varied. Another solution to $\partial E_-/\partial\beta = 0$ follows from the condition $(b_2 - 2b_1)\beta^2 + (-b_2 + 2\zeta) = 0$ (see eq. A.4). The deformation β_i then equals $\pm\sqrt{N/(N+2)}$ and ϵ_i (A.8) becomes zero.

References

- [1] F. Iachello and A. Arima, The interacting boson model (Cambridge University Press, Cambridge, 1987).
- [2] J.N. Ginocchio and M.W. Kirson, Phys. Rev. Lett. 44 (1980) 1744.
- [3] A.E.L. Dieperink, O. Scholten and F. Iachello, Phys. Rev. Lett. 44 (1980) 1747.
- [4] A. Bohr and B. Mottelson, Phys. Scripta 22 (1980) 468.
- [5] D.H. Feng, R. Gilmore and S.R. Deans, Phys. Rev. C 23 (1981) 1254.
- [6] E. López-Moreno and O. Castaños, Phys. Rev. C 54 (1996) 2374.
- [7] J. Jolie et al., Phys. Rev. Lett. 89 (2002) 182502.
- [8] F. Iachello and N.V. Zamfir, Phys. Rev. Lett. 92 (2004) 212501.
- [9] A. Leviatan, Phys. Rev. C 74 (2006) 051301(R).
- [10] R. Gilmore and D.H. Feng, Phys. Lett. B 76 (1978) 26.
- [11] D.H. Feng, R. Gilmore and L.M. Narducci, Phys. Rev. C 19 (1979) 1119.
- [12] P.D. Duval and B.R. Barrett, Phys. Lett. B 100 (1981) 223.
- [13] P.D. Duval and B.R. Barrett, Nucl. Phys. A 376 (1982) 213.
- [14] A. Frank, P. Van Isacker and C.E. Vargas, Phys. Rev. C 69 (2004) 034323.
- [15] A. Frank, P. Van Isacker and F. Iachello, Phys. Rev. C 73 (2006) 061302.
- [16] D.D. Warner and R.F. Casten, Phys. Rev. C 28 (1983) 1798.
- [17] K. Heyde et al., Nucl. Phys. A 466 (1987) 189.
- [18] R. Gilmore, Catastrophe theory for scientists and engineers (Wiley, New York, 1981).
- [19] R. Gilmore, Jour. Math. Phys. 20 (1979) 891.
- [20] A.E.L. Dieperink and O. Scholten, Nucl. Phys. A 346 (1980) 125.
- [21] A. Fossion et al., Nucl. Phys. A 697 (2002) 703.
- [22] M. Plischke and B. Bergersen, Equilibrium statistical physics (World Scientific, Singapore, 1994).